PCCP

PAPER

View Article Online
View Journal | View Issue

Cite this: *Phys. Chem. Chem. Phys.*, 2015, **17**, 16428

Hydroxylation of a metal-supported hexagonal boron nitride monolayer by oxygen induced water dissociation

Yufeng Guo* and Wanlin Guo

Received 29th April 2015,
Accepted 19th May 2015

DOI: 10.1039/c5cp02494c

www.rsc.org/pccp

Hydroxylated hexagonal boron nitride (h-BN) nanosheets exhibit potential application in nanocomposites and functional surface coating. Our first-principles calculations reveal possible hydroxylation of a h-BN monolayer on a Ni substrate by surface O adatom induced spontaneous dissociation of water molecules. Here one H atom is split from a water molecule by bonding with the O adatom on the B atom and the resulting O–H radical then bonds with an adjacent B atom, which leads to two hydroxyl groups formed on h-BN/Ni. Hydroxylation slightly influences the electronic properties of a Ni-supported h-BN layer. Similar water dissociation and hydroxylation can occur on the surface of O functionalized h-BN/Cu depending on the O adsorption configuration. Metal substrates play an important catalytic role in enhancing the chemical reactivity of O adatoms on h-BN with water molecules through transferring additional charges to them.

1. Introduction

Two-dimensional (2D) materials such as graphene, hexagonal boron nitride, and transition metal dichalcogenides and oxides comprised of one or a few atomic layers have attracted tremendous scientific interest and hold great promise for application in future functional devices. Due to a high surface-to-volume ratio, surface functionalization is a feasible way to alter and tailor 2D materials' properties and behaviors,[1,2] while the functionalizing process is also of broad interest in comprehending the chemistry of 2D materials. Hexagonal boron nitride (h-BN) is a graphene-like 2D material with the same honeycomb plane but alternating B and N atoms in the hexagonal lattice, possessing excellent mechanical properties,[3–5] high thermal conductivity[6,7] and outstanding chemical stability.[8–11] The h-BN nanosheet is a wide bandgap insulator,[12] whereas surface hydrogenation, fluorination, decorating and doping significantly modulate the electronic and magnetic properties of h-BN nanosheets.[13–18] The ability to chemically functionalize h-BN has massively expanded its potential for electronics and spintronics applications. Moreover, hydroxylation of h-BN nanosheets has been recently realized by oxygen radical functionalization with subsequent hydrolytic defunctionalization,[19] air-plasma[20] and ultrasonic treatments.[21] Grafted hydroxyl groups can drastically change the surface chemistry of h-BN and the resulting hydroxyl functionalized BN nanosheets are expected to be employed as mechanical enhancement elements in polymer nanocomposites[19] or super-hydrophilic surface coating.[20]

Water dissociation on metal oxide and the subsequent formation of hydroxyl groups on surfaces are extensively studied and confirmed by experimental and theoretical studies,[22–26] which can also be considered as a valuable route to conduct surface hydroxylation in a green manner with less pollution of the environment. In such a hydroxylation process, surface oxygen sites play a key role in the dissociation of water molecules. Recently, uniform and high-quality h-BN nanosheets have been successfully achieved on transition metal and Cu substrates[27–30] by chemical vapor deposition methods. The metallic substrates are important catalysts for synthesizing h-BN nanosheets, and could also affect their electronic properties and chemical reactivity.[31–33] Meanwhile, the BN nanosheet and its supporting metal substrate can be considered as a heterogeneous structure. To impart more functionality to this kind of BN/metal structure is highly advantageous and attractive for the development of BN based devices. Atomic oxygen can stably adsorb on the free-standing[34] or metal supported h-BN nanosheets.[17] Further study on the interaction of water molecules with surface O adatoms will be helpful for a better understanding of surface chemistry of the BN/metal heterogeneous system.

In this study, we have extensively investigated water dissociation on an O functionalized h-BN monolayer on a Ni substrate by first-principles calculations. A water molecule is split into one H atom bonding with the adsorbed O of h-BN where the O atom is on the top of the B atom or on the bridge site of the B–N bond. Two hydroxyl groups (O–H) are finally formed on the B atoms. The water

State Key Laboratory of Mechanics and Control of Mechanical Structures and MOE Key Laboratory for Intelligent Nano Materials and Devices, Institute of Nanoscience, Nanjing University of Aeronautics and Astronautics, Nanjing, 210016, China. E-mail: yfguo@nuaa.edu.cn; Fax: +86-25-84895827; Tel: +86-25-84890513

dissociation and hydroxylation process is spontaneous and exothermic because of high chemical activity of the O adatom induced by charge transfer from the Ni substrate and the strong interaction between the BN layer and Ni. The formed hydroxyl groups slightly influence the electronic properties of h-BN on the Ni substrate. Similar hydroxylation has also been observed for the O functionalized h-BN monolayer on Cu, but its reaction activity is lower than that on the Ni substrate.

2. Model and method

We chose a rhombus unit cell with a lattice length of 0.992 nm where a 4×4 h-BN monolayer (32 atoms) is placed on a 4×4 Ni(111) substrate. The Ni(111) substrate (80 atoms) is composed of five layers and atoms in the bottom layer are fixed during structural relaxation. The lattice parameter of h-BN in the experimental results is 0.252 nm.[35] To match with the Ni substrate, the lattice of the h-BN monolayer is compressed to 1.6%. There is a 2.2 nm vacuum region perpendicular to the plane of h-BN/Ni. All our computations were performed within the framework of density-functional theory (DFT) as implemented in the VASP code by using the projector augmented wave method with the Perdew–Burke–Ernzerhof (PBE) exchange–correlation functional.[36–38] The influence of van der Waals interactions is considered by choosing a modified version of vdW-DF, referred to as "optB86b-vdW", in which the revPBE exchange functional of the original vdW-DF of Dion *et al.*, is replaced with the optB86b exchange functional to yield more accurate equilibrium interatomic distances and energies for a wide range of systems.[39,40] All considered systems were firstly relaxed by using a conjugate-gradient algorithm until the force on each atom was less than 0.1 eV nm^{-1}. After structural relaxation, more exact calculations on energy were conducted with an energy cutoff of 500 eV and special k points sampled on a $6 \times 6 \times 1$ Monkhorst–Pack mesh.[41] Our calculations showed that the band structure and the energy gap of the h-BN monolayer are slightly affected by the 1.6% compressive strain. As the spin polarization effect slightly influences the electronic properties of the h-BN monolayer on the Ni substrate,[33] our calculations were conducted under spin-unresolved conditions. We created a large number of starting geometries by placing a water molecule in different nonequivalent positions on the O functionalized h-BN/Ni surface. The starting structures were optimized without any geometry constraints.

3. Results and discussion

For an h-BN monolayer on a Ni substrate, our calculations show that the equilibrium interlayer distance between the BN layer and Ni is 0.205 nm. There are two stable adsorption sites for an O atom on h-BN/Ni. One is O bonding on the top of the B atom and another is O bonding on the bridge site of the B–N bond. In the first case, the length of the B–O bond is 0.135 nm, and in the latter the lengths of B–O and N–O bonds are 0.148 and 0.154 nm, respectively. We calculate the binding energy E_b of the O atom with the Ni-supported h-BN monolayer by $E_b = E_{tot} - E_O - E_{BN/Ni}$, here E_{tot} is the total energy, $E_{BN/Ni}$ is the energy of the h-BN/Ni system after interacting with the O atom, and E_O is the energy of a single O atom calculated in a spin-resolved manner. The binding energies for O on the B atom and the B–N bond are −5.57 and −2.21 eV, respectively. The O atom on the top of the B atom is more stable than that on the B–N bond. The values of binding energies are different from that presented in ref. 33 because we considered the van der Waals interactions in both structural relaxation and total energy calculations, and selected the energy of the h-BN/Ni system after interacting with the O atom as $E_{BN/Ni}$. When we choose the energy of the noninteracting h-BN/Ni system as $E_{BN/Ni}$ and the van der Waals interaction is not included, the binding energy for O on the B atom is −3.70 eV, which is consistent with ref. 33. Moreover, the equilibrium interlayer distance between the h-BN layer and Ni decreases to 0.201 nm when the O atom bonds with the B atom, but increases to 0.288 nm when bonding with the B–N bond. The corresponding interlayer cohesive energies E_c ($E_c = E_{tot} - E_{BNO} - E_{Ni}$, E_{BNO} is the energy of the O functionalized h-BN monolayer and E_{Ni} is the energy of the Ni substrate) for the two cases are −0.56 and −0.14 eV per B–N pair, respectively. Surface oxygen functionalization could remarkably modify the interlayer distance and the interaction between the h-BN monolayer and its supporting substrate. Recent experiments[42,43] have shown that under slight oxidation conditions oxygen atoms and molecules can adsorb on the surface of h-BN nanosheets and form B–O bonds without causing any dramatic morphology change in the BN nanosheets, so the bonding of oxygen on the B atom or the B–N bond of the h-BN nanosheets presented in our theoretical model could be experimentally realizable.

For a water molecule in different starting structures on the O functionalized h-BN/Ni system, it is found that two hydroxyl groups finally form on two adjacent B atoms of the h-BN layers after complete structural relaxations. To better understand this chemical reaction and its intermediates, we calculated and recorded the total energies at different reaction stages. The energy change ΔE relative to the starting state and the corresponding initial, intermediate and final configurations are shown in Fig. 1 and 2. In the case of O on the top of the B atom (Fig. 1), the water molecule is first split into H and O–H. Then the dissociated H atom bonds with the O adatom and the O–H radical bonds with another adjacent B atom. In another case (Fig. 2), the approaching of water molecules towards the adsorbed O will weaken the N–O bond and facilitate the O atom moving towards the B atom. After this intermediate state had been reached, the water molecule incorporating with the O adatom will split into two hydroxyl groups, which is the same as that shown in Fig. 1b. The interlayer distance between the hydroxylated h-BN layer and the underlying Ni substrate is 0.2 nm. To compare the reaction activity, we calculate the reaction energy E_r ($E_r = E_{2OH/BN/Ni} - E_{BNO/Ni} - E_w$, here $E_{2OH/BN/Ni}$ is the total energy after hydroxylation, $E_{BNO/Ni}$ is the energy of O functionalized h-BN/Ni, and E_w is the energy of a water molecule) of −2.81 eV for the case that O on the top of the B atom and −6.42 eV for the case that O on the B–N bond. The difference in reaction energies due to the system of O on the top of the B atom is more stable than that system of O on the B–N bond. As shown in Fig. 1a and 2a, the water dissociation

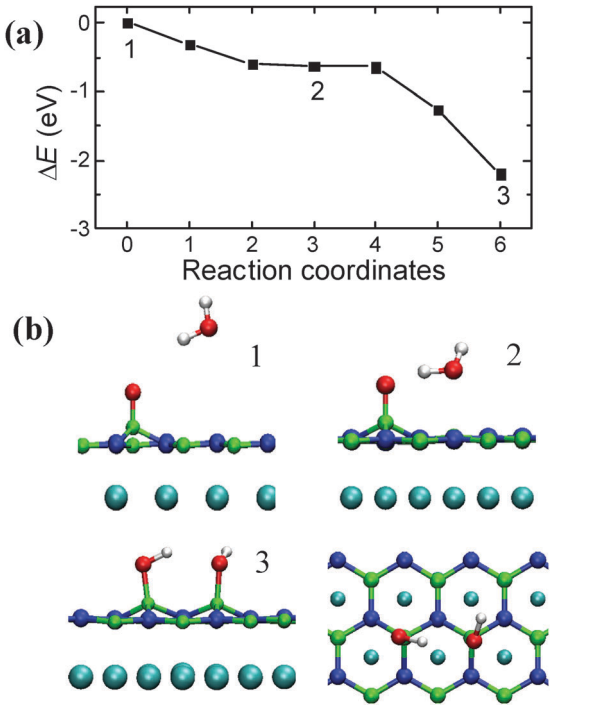

Fig. 1 Dissociation of a water molecule on the O functionalized h-BN/Ni system for O on the top of the B atom. (a) The energy change ΔE relative to the starting state at different reaction stages, and (b) the corresponding starting, intermediate and final stable configurations. The red, green, blue, white and cyan dots are oxygen, boron, nitrogen, hydrogen and nickel atoms, respectively.

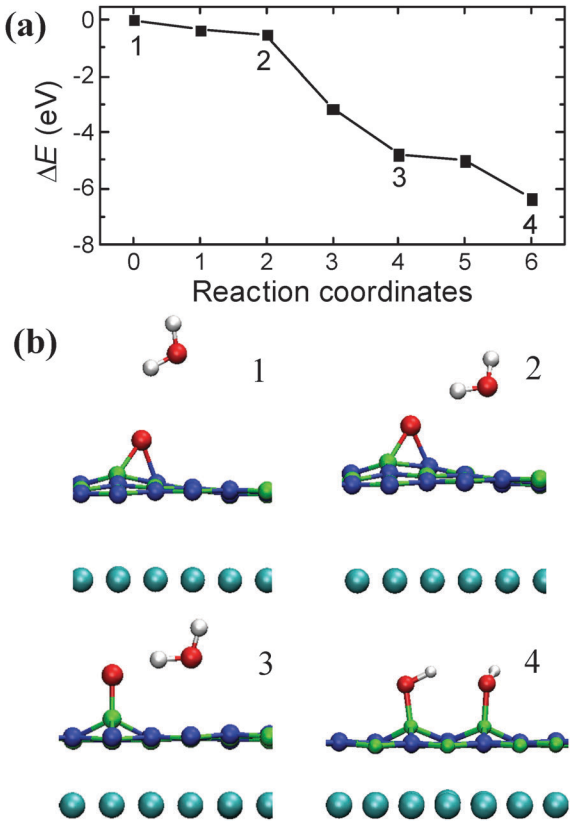

Fig. 2 Dissociation of a water molecule on the O functionalized h-BN/Ni system for O on the bridge site of the B–N bond. (a) The energy change ΔE relative to the starting state at different reaction stages, and (b) the corresponding starting, intermediate and final stable configurations. The red, green, blue, white and cyan dots are oxygen, boron, nitrogen, hydrogen and nickel atoms, respectively.

and surface hydroxylation in these two cases are all spontaneous and exothermic with total energy decreasing. The water molecule is energetically favorable to firstly react with the O site, and there will be a high energy barrier for direct splitting of H_2O into O–H and H on the surface of h-BN/Ni. Therefore, the chemical reaction of water dissociation prefers to be conducted using the Eley–Rideal (ER) mechanism.

The effects of hydroxylation on the electronic properties of the h-BN layer are presented by the local density of states (LDOS) of B, N and O atoms in Fig. 3. For an h-BN monolayer on Ni, there is a small peak at the Fermi level for the N atom because of a weak doping from the Ni substrate. After two hydroxyl groups formed on h-BN/Ni, the LDOS of the B and N atoms around the Fermi level are slightly changed as shown in Fig. 3b. However, the LDOS of the B, N and O atoms of the hydroxylated h-BN layer significantly increase at the Fermi level when the Ni substrate is removed (Fig. 3c). This means that surface hydroxylation slightly influences the electronic properties of the Ni-supported h-BN layer and the Ni substrate is a determinant factor in preserving the insulating nature of the h-BN layer.

Fig. 4a shows the LDOS of the O adatoms of the Ni-supported h-BN layer bonding with the B atom and the B–N bond. There is a peak appearing near the Fermi level for O on the B atom. After the formation of a hydroxyl, the peak of the LDOS for this O atom disappears (Fig. 3b). Similarly, the LDOS of the H atom in a water molecule also exhibits a small peak near the Fermi level (the inset in Fig. 4a), and it disappears when bonding with the O site.

The local states around the Fermi level are directly related to the chemical activity. To elucidate the role of the Ni substrate in the dissociation of water molecules, we calculate the charge density difference $\Delta\rho = \rho_{tot} - \rho_{BNO} - \rho_{Ni}$, here ρ_{tot} is the total charge density of O functionalized h-BN/Ni, ρ_{BNO} is the charge density of the O functionalized h-BN layer, and ρ_{Ni} is the charge density of the Ni substrate. Negative $\Delta\rho$ denotes charge depletion and positive for charge accumulation. Contour plots of $\Delta\rho$ for O on the top of the B atom and on the B–N bond are shown in Fig. 4b. Obvious charge accumulation transferred from the Ni substrate is observed on the O site when the O atom bonds only with the B atom. Larger charge accumulation indicates higher activity to bond with the H atom of water molecules, so the Ni substrate significantly enhances the chemical reactivity of this O site. In contrast, there is approximately no charge exchange between the Ni substrate and the O functionalized BN layer because of a large interlayer distance and only a very slight charge accumulation observed for O on the B–N bond. Furthermore, to better understand the interaction between the water molecule and the O adatom, we present in Fig. 4c the charge densities of the bands of O functionalized h-BN/Ni with an energy of 0.2 eV higher than the Fermi level (unoccupied bands) and a single water molecule with an energy of 1.0 eV lower than the Fermi level (occupied bands).

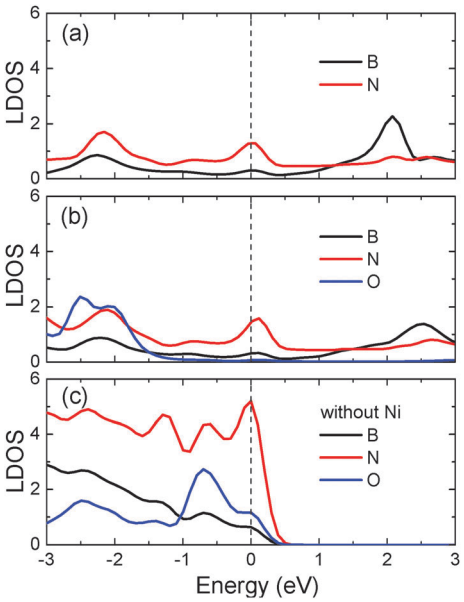

Fig. 3 The LDOS (in units of states per atom) of (a) the B and N atoms of an h-BN monolayer adsorbed on the Ni substrate, (b) the B, N and O atoms of two hydroxyl group functionalized h-BN/Ni and (c) the B, N and O atoms of the corresponding hydroxylated h-BN without the Ni substrate. The Fermi level is set to zero.

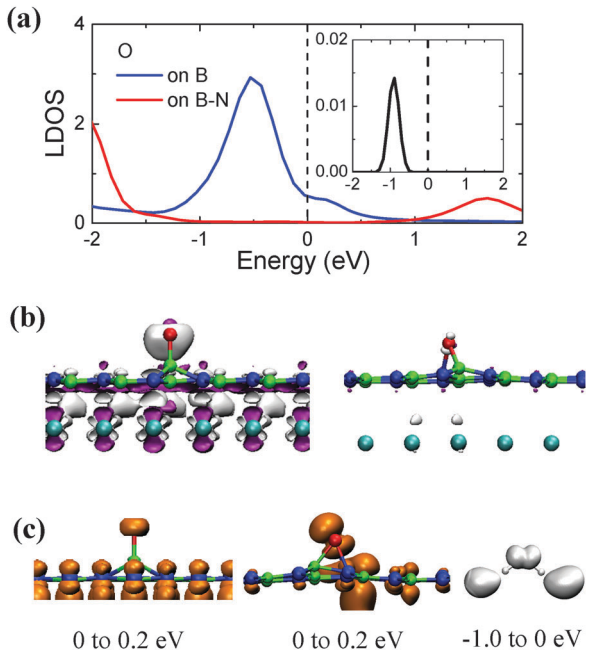

Fig. 4 (a) The LDOS (in units of states per atom) of the O atom bonding with the B atom and the B–N bond, and the inset shows the LDOS of the H atom of the water molecule. The Fermi level is set to zero. (b) Contour plots of the charge density difference $\Delta\rho$ [in units of 0.02 e Å^{-3}] of O functionalized h-BN/Ni with O on the top of the B atom and on the B–N bond. Here positive $\Delta\rho$ (white color) represents charge accumulation, and negative (purple color) represents charge depletion. (c) The corresponding isosurfaces of the charge densities of the bands [in units of 0.005 e Å^{-3}] of the O functionalized Ni/h-BN with O on the top of the B atom and on the B–N bond, and a single water molecule. Here the dot denotation is the same as that shown in Fig. 1. For clarity, the Ni substrates in (c) are not shown.

The energy bands below or above the Fermi level are directly related to the capability of chemical reactivity. It can be seen from Fig. 4c that the unoccupied bands distribute around the O sites, but more concentrated for O on the top of the B atom. For a water molecule, some occupied bands distribute around the H atoms, which could play a role in electron donation. When a water molecule interacts with the O atom on the bridge site of the B–N bond, some charges transfer to the O atom. The additional electrons firstly drive the O atom moving towards the B atom, the intermediate state shown in Fig. 2b, and then the dissociation of a water molecule occurs. A necessary condition for water dissociation is that there must be a dissociated O site available for bonding with the dissociated H and another unoccupied B atom to bond with the O–H radical. No water dissociation occurs when all B atom are unoccupied.

In contrast to atomic O, oxygen molecules are more popular and easier to obtain. So we have also studied water dissociation on O_2 functionalized h-BN/Ni by using the same method. According to the calculations of the DFT technique based nudged elastic band method,[44] it is shown in Fig. 5a that the adsorption of an O_2 molecule on h-BN/Ni is energetically favorable. The most favorable adsorption configuration is O_2 molecule bonding with two B atoms (the middle inset in Fig. 5a), where the O–O bond of the O_2 molecule is stretched to 0.151 nm. The length of the corresponding B–O bond is 0.149 nm larger than that of single O on the top of the B atom, and the binding energy E_b ($E_b = E_{tot} - E_{O_2} - E_{BN/Ni}$, here E_{tot} is the total energy, $E_{BN/Ni}$ is the energy of the noninteracting h-BN/Ni system, and E_{O_2} is the energy of an O_2 molecule) of the O_2 molecule with h-BN/Ni is −2.12 eV per molecule. The water molecule cannot dissociate on this O_2 functionalized h-BN/Ni. However, the adsorbed O_2 will dissociate and transform into a vertical O–B adsorption configuration after overcoming an energy barrier of 0.83 eV (Fig. 5a) where two O atoms bond with

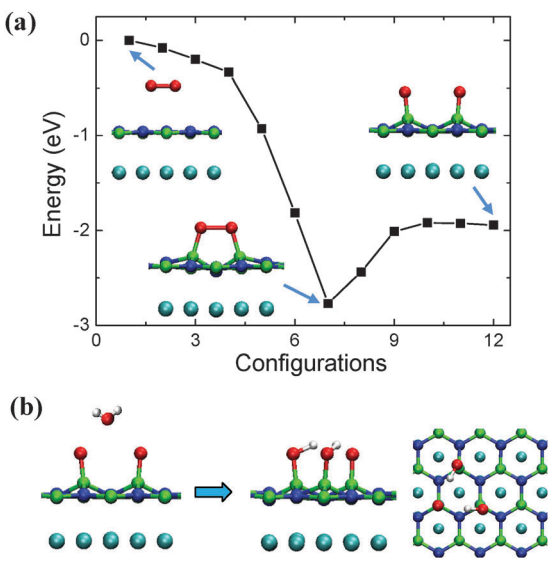

Fig. 5 (a) Minimum energy pathway of an O_2 molecule bonding with two B atoms of h-BN/Ni and dissociating into two separated O atoms. The insets show starting, most stable and dissociated O_2 structures. (b) A water molecule dissociation on the 2O functionalized h-BN/Ni system.

two nearest B atoms. Although the stability of such O–B adsorption is low (the reverse energy barrier is only 0.024 eV), we demonstrate by structural relaxation and total energy calculations that a water molecule spontaneously dissociates on the O site and two hydroxyl groups form on the h-BN surface, as shown in Fig. 5b. Another rest O site will lead to other water molecule dissociation. These results demonstrate that it is feasible to directly utilize oxygen molecules and water under appropriate conditions to obtain hydroxylated h-BN on the Ni substrate. It should be mentioned that water molecules cannot dissociate when the surface of h-BN/Ni is fully occupied by the O_2 molecules as no B atom is available for bonding with the O–H radical.

Moreover, in order to understand the effects of the substrate, we have studied water dissociation on O functionalized h-BN/Cu by using the same method. Here the lattice of the h-BN monolayer is stretched to 1.3% to match with the Cu substrate. There are two stable O adsorption sites: one is vertical on the B atom and another is on the B–N bond. The O binding energies on the B atom and the B–N bond are −5.29 eV and −3.29 eV, respectively. Similar to the case of h-BN/Ni, the water molecule spontaneously splits on the O site and becomes two hydroxyl groups when O is on the top of the B atom. The whole process of this reaction is exothermic with total energy decreasing. However, the O atom bonding with the B–N bond cannot cause the dissociation of water molecules. According to the minimum energy pathway,[44] it is shown in Fig. 6 that there will be an energy barrier of 0.77 eV to transform into 2OH functionalized h-BN/Cu. To explain the difference in chemical reaction with water on Ni and Cu substrates, Fig. 7 shows the charge density difference $\Delta\rho$ ($\Delta\rho = \rho_{tot} - \rho_{BNO} - \rho_{Cu}$) of O functionalized h-BN/Cu. Obviously, the interlayer charge exchanges between the O adsorbed h-BN layer and Cu are weaker than that with Ni for both cases that O on the top of the B atom and on the B–N bond. The corresponding equilibrium interlayer distances between the h-BN layer and the Cu substrate after O adsorption are 0.28 and 0.32 nm, respectively. Due to a larger interlayer distance and less charge transfer, the catalytic influence of Cu is weaker than that of Ni. Without the Ni or Cu substrate, the vertical O–B bond is not stable and no water dissociation is observed on the O functionalized h-BN layer. Therefore, the metal substrate plays a key catalytic role in oxygen induced water dissociation by providing additional electrons.

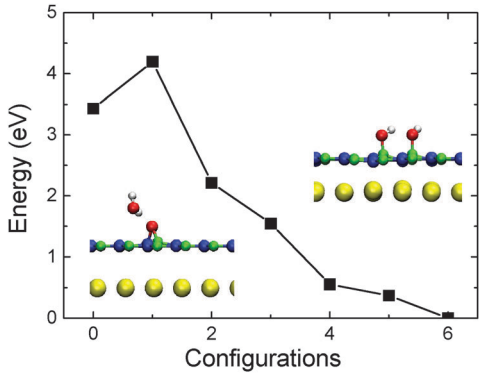

Fig. 6 Minimum energy pathway of a water molecule adsorbing on the O functionalized h-BN/Cu with O on the B–N bond and dissociating into two hydroxyl groups. The inset shows the initial (left) and final (right) structures. The red, green, blue, white, cyan and yellow dots are oxygen, boron, nitrogen, hydrogen, nickel and copper atoms, respectively.

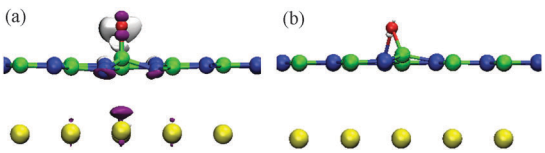

Fig. 7 Contour plots of the charge density difference $\Delta\rho$ [in units of 0.02 e Å^{-3}] of O functionalized h-BN/Cu with O (a) on the top of the B atom and (b) on the B–N bond. Here positive $\Delta\rho$ (white color) represents charge accumulation, and negative (purple color) represents charge depletion. The dot denotation is the same as that shown in Fig. 6.

4. Conclusions

In summary, our DFT calculations reveal hydroxylation of the h-BN layer on the Ni substrate by dissociation of water molecules on the surface O adatom. One H atom of the water molecule bonds with the O adatom and the resulting O–H radical bonds with an adjacent B atom. This leads to two hydroxyl groups formed on h-BN/Ni. Similar water dissociation and hydroxylation can occur on O functionalized h-BN/Cu depending on the O adsorption configuration. The metal substrates are essential catalysts for this hydroxylation process and enhance the chemical reactivity by transferring charges to the O sites. Our results highlight a possible way to achieve hydroxylated h-BN on metal substrates by using oxygen and water that are abundant and easily obtained from natural sources.

Acknowledgements

This work is supported by Program for New Century Excellent Talents in University (NCET-13-0855), the 973 Program (2013 CB932604, 2012CB933403), the NSF (11072109, 11472131), the Jiangsu NSF (BK20131356), the Fundamental Research Funds for the Central Universities (NE2012005, NJ20150048) of China, and the Research Fund of State Key Laboratory of Mechanics and Control of Mechanical Structures (Nanjing University of Aeronautics and Astronautics) (0413G01, MCMS-0414G01), a Project Funded by the Priority Academic Program Development of Jiangsu Higher Education Institutions, and sponsored by the Qing Lan Project.

References

1 S. Stankovich, D. A. Dikin, G. H. Dommett, K. M. Kohlhaas, E. J. Zimney, E. A. Stach, R. D. Piner, S. T. Nguyen and R. S. Ruoff, *Nature*, 2006, **442**, 282–286.
2 T. Ramanathan, A. Abdala, S. Stankovich, D. Dikin, M. Herrera-Alonso, R. Piner, D. Adamson, H. Schniepp, X. Chen and R. S. Ruoff, *Nat. Nanotechnol.*, 2008, **3**, 327–331.
3 R. C. Andrew, R. E. Mapasha, A. M. Ukpong and N. Chetty, *Phys. Rev. B: Condens. Matter Mater. Phys.*, 2012, **85**, 125428.

4 L. Boldrin, F. Scarpa, R. Chowdhury and S. Adhikari, *Nanotechnology*, 2011, **22**, 505702.
5 H. Şahin, S. Cahangirov, M. Topsakal, E. Bekaroglu, E. Akturk, R. T. Senger and S. Ciraci, *Phys. Rev. B: Condens. Matter Mater. Phys.*, 2009, **80**, 155453.
6 C. Sevik, A. Kinaci, J. B. Haskins and T. Çağın, *Phys. Rev. B: Condens. Matter Mater. Phys.*, 2011, **84**, 085409.
7 J. W. Jiang, J. S. Wang and B. S. Wang, *Appl. Phys. Lett.*, 2011, **99**, 043109.
8 J. Yu, L. Qin, Y. Hao, S. Kuang, X. Bai, Y. M. Chong, W. Zhang and E. Wang, *ACS Nano*, 2010, **4**, 414–422.
9 K. Simonov, N. A. Vinogradov, M. L. Ng, A. Vinogradov, N. Mårtensson and A. Preobrajenski, *Surf. Sci.*, 2012, **606**, 564–570.
10 L. H. Li, J. Cervenka, K. Watanabe, T. Taniguchi and Y. Chen, *ACS Nano*, 2014, **8**, 1457–1462.
11 Z. Liu, Y. Gong, W. Zhou, L. Ma, J. Yu, J. C. Idrobo, J. Jung, A. H. MacDonald, R. Vajtai, J. Lou and P. M. Ajayan, *Nat. Commun.*, 2013, **4**, 2541.
12 D. Golberg, Y. Bando, Y. Huang, T. Terao, M. Mitome, C. Tang and C. Zhi, *ACS Nano*, 2010, **4**, 2979–2993.
13 W. Chen, Y. Li, G. Yu, C. Z. Li, S. B. Zhang, Z. Zhou and Z. Chen, *J. Am. Chem. Soc.*, 2010, **132**, 1699–1705.
14 Z. H. Zhang, X. C. Zeng and W. L. Guo, *J. Am. Chem. Soc.*, 2011, **133**, 14831–14838.
15 B. Huang, H. Xiang, J. Yu and S. H. Wei, *Phys. Rev. Lett.*, 2012, **108**, 206802.
16 M. Du, X. Li, A. Wang, Y. Wu, X. Hao and M. Zhao, *Angew. Chem., Int. Ed.*, 2014, **53**, 3645–3649.
17 Y. F. Guo and W. L. Guo, *Nanoscale*, 2014, **6**, 3731–3736.
18 Y. F. Guo and W. L. Guo, *J. Phys. Chem. C*, 2015, **119**, 873–878.
19 T. Sainsbury, A. Satti, P. May, Z. Wang, I. McGovern, Y. K. Gunko and J. Coleman, *J. Am. Chem. Soc.*, 2012, **134**, 18758–18771.
20 A. Pakdel, Y. Bando and D. Golberg, *ACS Nano*, 2014, **8**, 10631–10639.
21 Y. R. Tang, D. W. Lin, Y. Gao, J. Xu and B. H. Guo, *Ind. Eng. Chem. Res.*, 2014, **53**, 4689–4696.
22 I. Brookes, C. Muryn and G. I. Thornton, *Phys. Rev. Lett.*, 2001, **87**, 266103.
23 R. Schaub, P. Thostrup, N. Lopez, E. Lægsgaard, I. Stensgaard, J. K. Nørskov and F. Besenbacher, *Phys. Rev. Lett.*, 2001, **87**, 266104.
24 O. Bikondoa, C. L. Pang, R. Ithnin, C. A. Muryn, H. Onishi and G. Thornton, *Nat. Mater.*, 2006, **5**, 189–192.
25 P. J. Lindan and C. Zhang, *Phys. Rev. B: Condens. Matter Mater. Phys.*, 2005, **72**, 075439.
26 S. Wendt, J. Matthiesen, R. Schaub, E. K. Vestergaard, E. Lægsgaard, F. Besenbacher and B. Hammer, *Phys. Rev. Lett.*, 2006, **96**, 066107.
27 Y. Shi, C. Hamsen, X. Jia, K. K. Kim, A. Reina, M. Hofmann, A. L. Hsu, K. Zhang, H. Li and Z. Y. Juang, *Nano Lett.*, 2010, **10**, 4134–4139.
28 T. Herden, M. Ternes and K. Kern, *Nano Lett.*, 2014, **14**, 3623–3627.
29 L. Song, L. Ci, H. Lu, P. B. Sorokin, C. Jin, J. Ni, A. G. Kvashnin, D. G. Kvashnin, J. Lou and B. I. Yakobson, *Nano Lett.*, 2010, **10**, 3209–3215.
30 X. Li, J. Yin, J. Zhou and W. Guo, *Nanotechnology*, 2014, **25**, 105701.
31 W. Auwarter, T. J. Kreutz, T. Greber and J. Osterwalder, *Surf. Sci.*, 1999, **429**, 229–236.
32 G. B. Grad, P. Blaha, K. Schwarz, W. Auwarter and T. Greber, *Phys. Rev. B: Condens. Matter Mater. Phys.*, 2003, **68**, 085404.
33 A. Lyalin, A. Nakayama, K. Uosaki and T. Taketsugu, *J. Phys. Chem. C*, 2013, **117**, 21359–21370.
34 Y. Zhao, X. Wu, J. Yang and X. C. Zeng, *Phys. Chem. Chem. Phys.*, 2012, **14**, 5545–5550.
35 C. S. Yoo, J. Akella, H. Cynn and M. Nicol, *Phys. Rev. B: Condens. Matter Mater. Phys.*, 1997, **56**, 140–146.
36 P. E. Blochl, *Phys. Rev. B: Condens. Matter Mater. Phys.*, 1994, **50**, 17953–17979.
37 G. Kresse and D. Joubert, *Phys. Rev. B: Condens. Matter Mater. Phys.*, 1999, **59**, 1758–1775.
38 J. P. Perdew, K. Burke and M. Ernzerhof, *Phys. Rev. Lett.*, 1996, **77**, 3865–3868.
39 J. Klimes, D. R. Bowler and A. Michelides, *J. Phys.: Condens. Matter*, 2010, **22**, 022201.
40 J. Klimes, D. R. Bowler and A. Michelides, *Phys. Rev. B: Condens. Matter Mater. Phys.*, 2011, **83**, 195131.
41 H. J. Monkhorst and J. D. Pack, *Phys. Rev. B: Condens. Matter Mater. Phys.*, 1976, **13**, 5188–5192.
42 L. H. Li, J. Cervenka, K. Watanabe, T. Taniguchi and Y. Chen, *ACS Nano*, 2014, **8**, 1457–1462.
43 K. A. Simonov, N. A. Vinogradov, M. L. Ng, A. S. Vinogradov, N. Mårtensson and A. B. Preobrajenski, *Surf. Sci.*, 2012, **606**, 564–570.
44 G. Mills, H. Jónsson and G. K. Schenter, *Surf. Sci.*, 1995, **324**, 305–337.